

Modulation of Inhibitory Transmission by Dopamine in Rat Basal Forebrain Nuclei: Activation of Presynaptic D₁-like Dopaminergic Receptors

Toshihiko Momiyama¹ and J. A. Sim²

¹Department of Pharmacology, University College London, London WC1E 6BT, United Kingdom, and ²Department of Neurobiology, Babraham Institute, Cambs CB2 4AT, United Kingdom

The effects of dopamine (DA) on inhibitory transmission onto identified magnocellular neurons were examined in rat basal forebrain slices using whole-cell recording. IPSCs evoked by focal stimulation within basal forebrain nuclei were reversibly blocked by 10 μ M bicuculline and had a decay time constant of 20.1 ± 0.77 msec in the presence of 6-cyano-7-nitroquinoxaline-2,3-dione (5 μ M). Bath application of DA reduced the amplitude of IPSCs up to $71.1 \pm 1.49\%$ in a concentration-dependent manner between 0.003 and 1 mM (the IC₅₀ value being 6.6 μ M), without any effect on the holding current at -70 mV. DA (10 μ M) reduced the frequency of miniature IPSCs (mIPSCs) recorded in the presence of TTX (0.5 μ M), without affecting their mean amplitude, rise time, and decay time constant. Furthermore, the DA-induced effect on mIPSCs remained unaffected by 100 μ M cadmium, suggesting

a presynaptic mechanism independent of calcium influx. SKF 81297, a D₁-like agonist, mimicked DA-induced effect on evoked IPSCs (IC₅₀, 10.9 μ M), whereas R(-)-TNPA or (-)-quinpirole, D₂-like agonists (30 μ M), had little or no effect on the amplitude of evoked IPSCs. R(+)-SCH 23390, a D₁-like antagonist, antagonized the DA-induced effect on IPSCs (K_B 0.82 μ M), whereas S(-)-eticlopride, a D₂-like antagonist, showed slight antagonism (K_B 7.8 μ M). Forskolin (10 μ M) reduced the amplitude of evoked IPSCs to $\sim 58\%$ of the control and occluded the inhibitory effect of DA. These findings indicate that DA reduces inhibitory transmission onto magnocellular basal forebrain neurons by activating presynaptic D₁-like receptors.

Key words: dopamine; D₁ receptor; inhibitory postsynaptic currents; magnocellular basal forebrain nuclei; presynaptic modulation

Magnocellular basal forebrain (MBF) neurons in the vertical and horizontal limbs of diagonal band of Broca (HDBB), substantia innominata (SI), and nucleus basalis (nB) form the principal source of cholinergic innervation to the cerebral and subcortical brain regions (Rye et al., 1984). Pathophysiologically, degeneration of these cholinergic neurons has been observed in patients with Alzheimer's disease (Coyle et al., 1983; Oyanagi et al., 1989), yet the question of how these cortically projecting neurons can be influenced remains to be clarified. Morphological studies using immunohistochemical techniques have demonstrated that the basal forebrain region receives dopaminergic fibers from the ventral tegmental area, substantia nigra pars compacta, and medial zona interna (Martinez-Murillo et al., 1988; Semba et al., 1988; Eaton et al., 1994). Despite these well documented pathways, the basic effects of dopamine (DA) on synaptic transmission within basal forebrain nuclei are still not well understood. Previous electrophysiological studies using anesthetized rats have shown that neuronal activity is variably inhibited or excited by iontophoretic application of DA in other groups of basal forebrain nuclei, namely the globus pallidus (Bergstrom and Walters, 1984) and ventral pallidum (Napier and Maslowski-Cobuzzi,

1994). Our recent studies (Momiyama et al., 1995a; 1996) showed that DA reduces excitatory synaptic transmission onto visualized magnocellular neurons within the HDBB, SI, and nB regions of the rat brain. Furthermore, our pharmacological studies revealed that the action of DA was mediated via the activation of presynaptically located D₁-like receptors. Similar reduction of excitatory transmission mediated by presynaptic D₁-like receptors has been reported in nucleus accumbens (Pennartz et al., 1992; Harvey and Lacey, 1996; Nicola et al., 1996). In contrast, information regarding the effect of DA on inhibitory synaptic transmission in basal forebrain is sparse, although it has been known that iontophoretic application of DA attenuated the inhibitory action of iontophoretically administered GABA on the firing rates of neurons within the globus pallidus (Bergstrom and Walters, 1984). To further understand the role of DA in basal forebrain nuclei, the present study examined the effect of DA on the inhibitory synaptic transmission onto visualized MBF neurons using the whole-cell patch-clamp technique in a thin-slice preparation of the rat brain. The identity of the DA receptor family involved was studied using pharmacologically selective agonists and antagonists.

Preliminary data from these studies have been published previously in abstract form (Momiyama et al., 1995b).

Received July 8, 1996; revised Sept. 10, 1996; accepted Sept. 16, 1996.

This work was supported by grants from The Wellcome Trust (T.M.) and the Medical Research Council (J.A.S.). We are grateful to Professor D. A. Brown (University College London) for his helpful discussion. We are also grateful to Dr. Stephen F. Traynelis (Emory University) for the software to analyze miniature IPSCs.

Correspondence should be addressed to Dr. Toshihiko Momiyama at his present address: Department of Physiology, Nagasaki University School of Medicine, 1-12-4 Sakamoto, Nagasaki 852, Japan.

Copyright © 1996 Society for Neuroscience 0270-6474/96/167505-08\$05.00/0

MATERIALS AND METHODS

Preparation and recording procedures. The details of slicing and whole-cell recording procedures were as described previously (Sim and Griffith, 1996). In brief, 12- to 14-d-old rats were decapitated after deep anesthesia with chloroform, and their brains were removed and placed in an ice-cold cutting Krebs solution of the following composition (in mM): 118 NaCl, 3 KCl, 0.5 CaCl₂, 6 MgCl₂, 25 NaHCO₃, 5 HEPES, and 11 D-glucose, continuously bubbled with 95% O₂/5% CO₂. Coronal slices

(200 μm) containing the basal forebrain region were prepared using a microslicer (Campden, Loughborough, UK) and incubated in normal Krebs solution of the following composition (in mM): 118 NaCl, 3 KCl, 2.5 CaCl_2 , 1.2 MgCl_2 , 25 NaHCO_3 , 5 HEPES, 11 D-glucose, pH 7.2, when bubbled with 95% O_2 /5% CO_2 at room temperature (20–23°C) in a temperature-controlled room for at least 1 hr. For recording, a slice was transferred to the recording chamber, held submerged, and superfused continuously with the normal Krebs solution (bubbled with 95% O_2 /5% CO_2) at a rate of 6 ml/min.

Patch electrodes were pulled from thin-walled borosilicate glass capillaries (1.5 mm outer diameter; Clark Electromedical, Reading, UK) and had resistances of 5–8 M Ω when filled with a potassium acetate-based internal solution of the following composition (in mM): 108 potassium acetate, 15.6 KCl, 40 HEPES, 1 MgCl_2 , 2 BAPTA, 4 Na_2GTP , 0.1 MgATP , 0.2 CaCl_2 (for nominal $[\text{Ca}^{2+}]_i$ of 30 nM, see Sim and Griffith, 1996), and pH adjusted to 7.2 with 12 mM NaOH. Whole-cell recordings were made using an Axopatch 200A (Axon Instruments, Foster City, CA) from visually identified MBF neurons viewed with the aid of a microscope (Microtec-2A, Micro Instruments, Oxford, UK) fitted with Hoffman-modulation optics. The morphological characteristics of these neurons were as follows: large diameter (>20 μm) of the soma, with a triangular, fusiform, or multipolar shape (Sim, 1994). Stimulating electrodes were pulled from theta glass (Clark Electromedical, Reading, UK) and filled with normal Krebs solution. Inhibitory synaptic responses were evoked by careful placement of a stimulating electrode within a 50–150 μm radius of the recorded cell (the mean distance between the stimulating electrode and the nearest edge of the recorded cell being $70.7 \pm 2.69 \mu\text{m}$; $n = 83$ cells). A voltage pulse (0.2–0.4 msec in duration) was applied at a frequency of 0.1 Hz with suprathreshold intensity. A glass bridge reference electrode containing 4% agar-saline was used as described previously (Sim and Griffith, 1996). Experiments were carried out at room temperature (20–26°C).

Data were collected (10 kHz sampling rate and low-pass-filtered at 3–10 kHz with an 8-pole Bessel filter) using pClamp6 (Axon Instruments) software and digitized at 10–20 kHz for computer analysis. Synaptic currents were routinely evoked at 0.1 Hz, and all traces shown are the averages of 10 traces, with their respective SD. In the present study, IPSCs are inwardly directing; the reversal potential for chloride ions was set at -54 mV , and recordings were made from a holding potential of -70 mV . For experiments studying mIPSCs, data were digitized continuously at 10–20 kHz and stored on a computer. mIPSCs were detected using software generously provided by Dr. Stephen F. Traynelis (Emory University, Atlanta, GA). Curve-fitting was carried out using “Graphpad Inplot” computer software (Graphpad, San Diego, CA). Data are expressed as mean \pm SEM. Statistical analysis was performed using Student's *t*-test (two-tailed) or a nonparametric Mann-Whitney test, where appropriate; $p < 0.05$ was considered statistically significant.

Drugs and their application. All drugs were bath-applied. Dopamine (Sigma, St Louis, MO), (\pm)-6-chloro-7,8-dihydroxy-1-phenyl-2,3,4,5-tetrahydro-1H-3-benzazepine hydrobromide (SKF 81297; Research Biochemicals, Natick, MA), R(-)-2,10,11-trihydroxy-N-propyl-noraporphine hydrobromide (TNPA; Research Biochemicals), *trans*-($-$)-4aR-4,4a,5,6,7,8,8a,9-octahydro-5-propyl-1H-pyrazolo[3,4-g]quinoline (($-$)-quinpirole), R(+)-7-chloro-8-hydroxy-3-methyl-1-phenyl-2,3,4,5-tetrahydro-1H-3-benzazepine hydrochloride (SCH 23390, Research Biochemicals), S(-)-3-chloro-5-ethyl-N-[(1-ethyl-2-pyrrolidinyl)methyl]-6-hydroxy-2-methoxy-benzamide hydrochloride (eticlopride; Research Biochemicals), bicuculline (Sigma), and tetrodotoxin (TTX; Sigma) were prepared as 10 mM stock solutions in distilled water and kept frozen. 6-cyano-7-nitroquinoxaline-2,3-dione (CNQX; Tocris Cookson, Bristol, UK), forskolin (Sigma), and 1,9-dideoxyforskolin (Sigma) were dissolved as 10 mM stock in dimethylsulfoxide (Sigma). Stock solutions were diluted to the final concentrations in normal Krebs solution just before each experiment. Antagonists were applied at least 10–15 min before the addition of agonist in the continuing presence of antagonist.

RESULTS

General properties of GABAergic IPSCs

In the present study, whole-cell recordings were made from 114 MBF neurons clamped at -70 mV (close to their resting membrane potential) (Sim and Griffith, 1996). The mean diameter of the long axis of the neurons was $29.7 \pm 0.42 \mu\text{m}$ (mean \pm SEM, $n = 104$), and the cell capacitance was $41.8 \pm 1.10 \text{ pF}$ ($n = 114$).

IPSCs were evoked in MBF neurons by focal stimulation in the

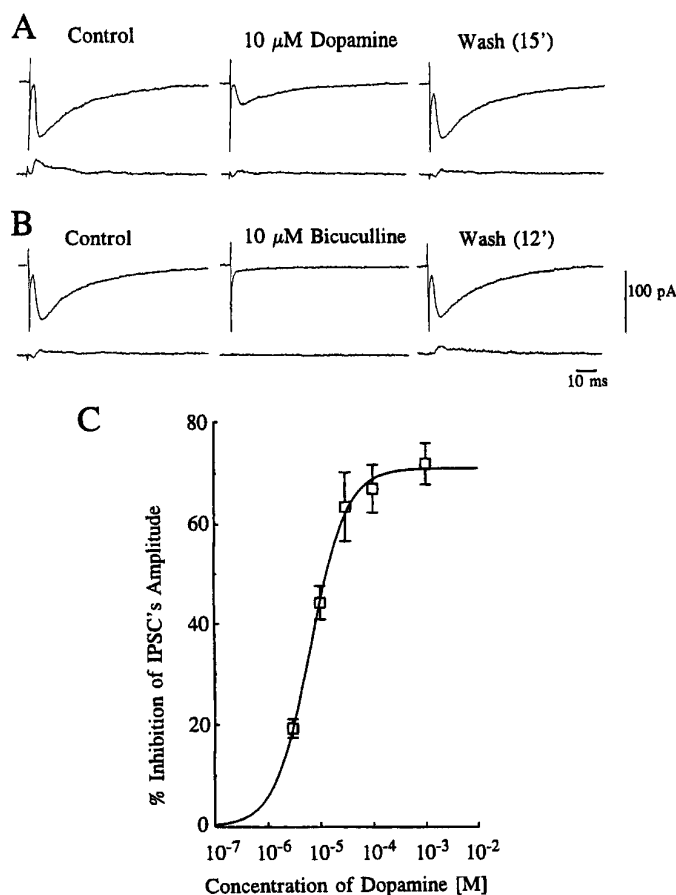


Figure 1. Inhibition of GABAergic IPSCs by dopamine. IPSCs were evoked at 0.1 Hz in the presence of CNQX (5 μM) to eliminate excitatory glutamatergic components. Traces in *A* and *B* show averaged records of 10 consecutive responses (top traces) with their corresponding SD (bottom traces). The holding potential was -70 mV . *A*, Bath application of dopamine (10 μM) produced a 61% reduction of the amplitude of evoked IPSCs in this cell after 3 min, and its effect was reversed after 15 min wash. *B*, Reversible suppression of IPSCs by a GABA_A receptor antagonist, bicuculline (10 μM), in the same cell, after recovery from DA-induced effect. The effect of bicuculline recovered after 12 min wash. Note that the IPSCs are depicted as inward currents, because the equilibrium potential for chloride ions was -54 mV , and cells held at -70 mV . *C*, Concentration-dependent inhibition of evoked IPSCs by DA. Each point shows the mean \pm SEM of data pooled from 4–19 cells. The estimated IC_{50} value, maximum inhibition, and Hill slope value were $6.6 \mu\text{M}$, $71.1 \pm 1.49\%$, and 1.28, respectively.

presence of 5 μM CNQX to eliminate excitatory components. In contrast to EPSCs, IPSCs were evoked less frequently (cf. Sim and Griffith, 1996) in MBF neurons, because the placement of the stimulating electrode seemed to be more critical in eliciting IPSCs than EPSCs. After successful placement of the stimulating electrode, IPSCs were evoked in an “all-or-none” manner around the threshold of stimulation intensity, suggesting that they were monosynaptic in origin (Stern et al., 1992; Takahashi, 1992; Jonas et al., 1993). The amplitude and time constant of the decay phase of evoked IPSCs in 82 neurons were $-86.4 \pm 6.52 \text{ pA}$ and $20.1 \pm 0.77 \text{ msec}$, respectively.

Effect of dopamine on evoked IPSCs

Figure 1*A* shows the effect of DA on the amplitude of evoked IPSCs recorded in the presence of 5 μM CNQX. Bath application of 10 μM DA (for 5 min) produced a gradual decline in the

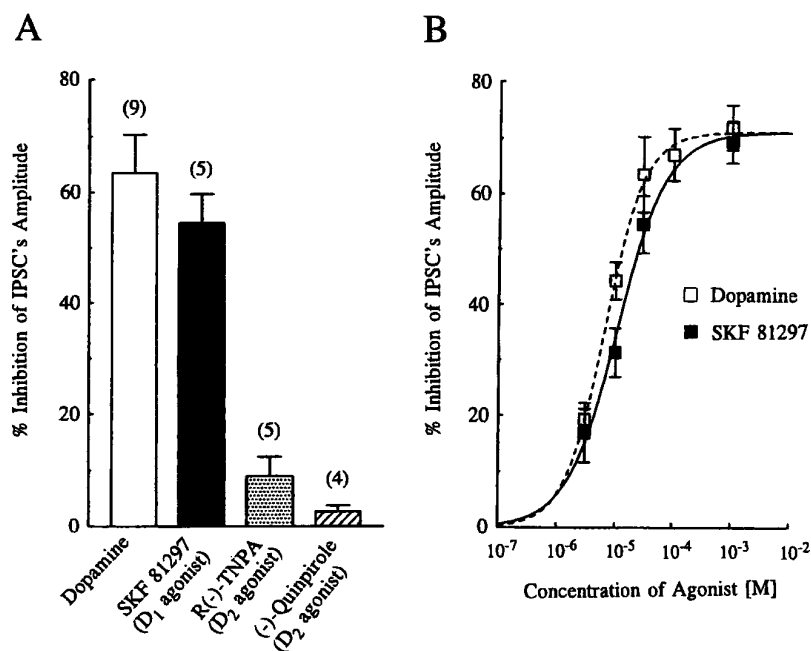


Figure 2. Effect of dopamine receptor agonists on evoked IPSCs. *A*, Summary histograms showing the mean \pm SEM of the inhibitory effects of DA (Dopamine), SKF 81297, R(-)-TNPA, and (-)-Quinpirole on the amplitude of evoked IPSCs. All agonists were applied at 30 μ M concentration. Values for DA, SKF 81297, R(-)-TNPA, and (-)-quinpirole were 63.5 \pm 6.8% ($n = 9$), 54.5 \pm 5.2% ($n = 5$), 8.9 \pm 3.5% ($n = 5$), and 2.6 \pm 1.1% ($n = 4$), respectively. (The value for DA was derived from the concentration–response curve in Fig. 1, and for SKF 81297 from the concentration–response curve in Fig. 2*B*.) Application of either R(-)-TNPA or (-)-quinpirole had little effect ($p < 0.01$) on inhibition of the amplitude of IPSCs, compared with DA or SKF 81297. The difference between DA and SKF 81297 or R(-)-TNPA and (-)-quinpirole was not significant ($p > 0.27$ or $p > 0.07$, respectively). *B*, Concentration–response curve for the inhibition of IPSC amplitude by DA (open squares, reproduced from Fig. 1) and SKF 81297 (closed squares). Each point represents the mean \pm SEM of pooled data from 3–19 cells. The estimated IC₅₀ value and Hill slopes for SKF 81297 were 10.9 μ M and 1.02, respectively. Note that the maximum effect of SKF 81297 was constrained to that of DA.

amplitude of the evoked IPSCs, reaching a maximum level 3 min after the onset of application. The effect of DA was reversed after 10–20 min washout. The GABAergic nature of these IPSCs was confirmed when they were reversibly blocked by bath application of 10 μ M bicuculline, a GABA_A receptor antagonist (Fig. 1*B*). DA-induced inhibitory effects on evoked IPSCs were concentration-dependent between 0.003 and 1 mM. Figure 1*C* depicts the concentration–response curve pooled from 47 neurons (Fig. 1*C*), giving an apparent IC₅₀ value, mean maximum effect, and Hill slope value of 6.6 μ M, 71.1 \pm 1.49%, and 1.28, respectively. No desensitization was observed when DA was applied repeatedly after 10–20 min washout intervals. DA applied at concentrations up to 1 mM had no effect on the holding current or decay time constant at a holding potential of -70 mV.

Pharmacology of DA-induced inhibition of evoked IPSCs

To investigate the subtypes of DA receptor mediating DA-induced inhibition of evoked IPSCs, we examined both the action of selective DA receptor agonists on the amplitude of evoked IPSCs (Fig. 2) and the effect of selective DA receptor antagonists on the concentration–response curve produced by DA (Fig. 3).

Effect of DA receptor agonists

Figure 2*A* summarizes the effect of DA agonists, applied at 30 μ M on the amplitude of evoked IPSCs, and data expressed as the mean percentage (\pm SEM) inhibition were depicted as histograms. Bath application of the selective D₁-like receptor agonist SKF 81297 (Andersen and Jansen, 1990) reduced the amplitude of evoked IPSCs by 54.5 \pm 5.2% ($n = 5$). In contrast, a D₂-like agonist R(-)-TNPA (Gao et al., 1990) had little or no effect on the amplitude of evoked IPSCs (8.9 \pm 3.5% reduction, $n = 5$). Similarly, another D₂-like receptor agonist, (-)-quinpirole (Titus et al., 1983), had little or no effect on the amplitude of evoked IPSCs (2.6 \pm 1.1%, $n = 4$) (Fig. 2*A*). SKF 81297 mimicked the effect of DA and also reduced the IPSC in a concentration-dependent manner between 0.003 and 1 mM (Fig. 2*B*). Pooled data from 16 cells yielded an apparent IC₅₀ value of 10.9 μ M and a Hill slope value of 1.02 (when the mean maximum effect was

constrained to that of DA). In addition, we also examined the effect of SKF 81297 in the presence of R(-)-TNPA (both applied at 30 μ M) but found no difference from the effect of SKF 81297 alone (data not shown).

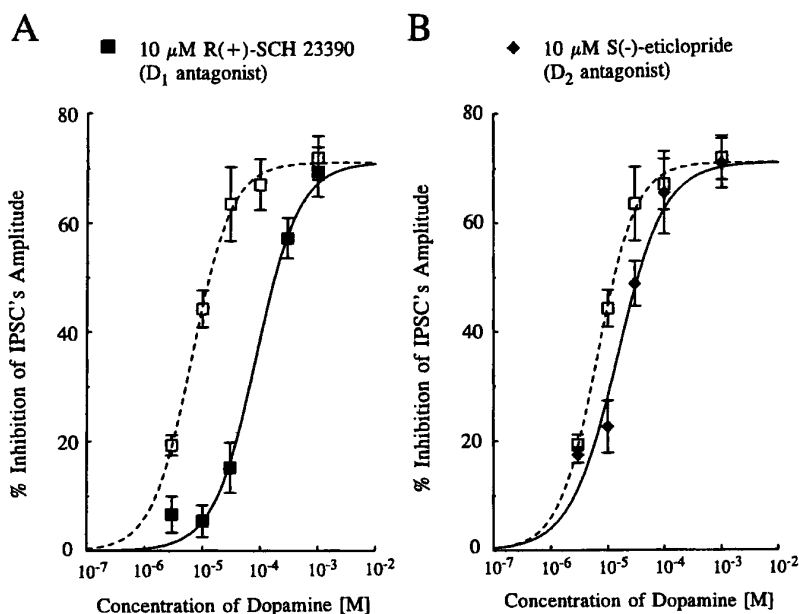
Effect of DA receptor antagonist on DA-induced inhibition of evoked IPSCs

The effects of a D₁-like receptor antagonist, R(+)-SCH 23390 (Iorio et al., 1983), and a D₂-like antagonist, S(-)-eticlopride (Hall et al., 1985), on the concentration-dependent inhibition curve for DA were examined (Fig. 3). Bath application of 10 μ M R(+)-SCH 23390 or S(-)-eticlopride alone had no effect on the holding current, amplitude, or time course of evoked IPSCs at -70 mV. In the presence of 10 μ M R(+)-SCH 23390, the concentration–response curve for DA was shifted to the right (Fig. 3*A*), whereas in the presence of S(-)-eticlopride (10 μ M) only a very small shift of the concentration–response curve was observed (Fig. 3*B*). Assuming that both R(+)-SCH 23390 and S(-)-eticlopride behave as competitive antagonists, apparent K_B values of 0.82 μ M (pK_B 6.1) and of 7.8 μ M (pK_B 5.1), respectively, were calculated using the equation of $K_B = [B]/(DR - 1)$, where $[B]$ is the concentration of the antagonist and DR (dose-ratio) is the ratio of the mean IC₅₀ values for pooled data in the presence and absence of antagonist.

Effect of forskolin and 1,9-dideoxyforskolin on evoked IPSCs

D₁-like receptors have been classified as those positively coupled with adenylate cyclase activity; therefore, we tested the effect of forskolin (which stimulates adenylate cyclase) on the inhibitory action of DA (Fig. 4). Bath application of forskolin (10 μ M) alone produced a gradual reduction in the amplitude of evoked IPSCs, reaching a steady level after 10–15 min (Fig. 4*A,C*). The mean percentage inhibition of evoked IPSCs by 10 μ M forskolin after a 15 min period was 42.1 \pm 6.8 ($n = 10$) (Fig. 4*B*). In contrast, 10 μ M 1,9-dideoxyforskolin, the inactive form of forskolin, had little or no effect (2.4 \pm 1.5%; $n = 5$) on the amplitude of evoked IPSCs (Fig. 4*A,B*). DA (10 μ M) applied after forskolin had reached its steady state produced no further effect on the amplitude of

Figure 3. Effects of dopamine receptor antagonists on dopamine-induced inhibition of evoked IPSCs. *A*, Concentration–response curves for IPSC inhibition by DA in the absence (*open squares*) and presence (*closed squares*) of 10 μM R(+)-SCH 23390 (a D_1 -like receptor antagonist). The resultant curve in the presence of R(+)-SCH 23390 was shifted to the right, with an IC_{50} value and Hill slope of 86.4 μM and 1.17, respectively. *B*, Concentration–response curves in the absence (*open squares*) and presence (*closed diamonds*) of S(-)-eticlopride (a D_2 -like antagonist). The resultant curve was shifted to the right to a small extent, in the presence of the D_2 -like antagonist; the estimated IC_{50} value and Hill slope were 15.0 μM and 0.97, respectively. All points depicted are the mean \pm SEM of pooled data from 3–19 cells. The maximum effect value in the presence of both antagonists was constrained to that observed in the absence of antagonist (i.e., 71.1%). Note that the concentration–response curves of DA alone (*open squares*) are the same as those depicted in Figure 1.



evoked IPSCs (Fig. 4*B,C*); however, the inhibitory effect of DA on the amplitude of evoked IPSCs was still apparent (although reduced) if applied before the effect of forskolin had reached its plateau (3–7 min after application of forskolin), showing that forskolin had indeed occluded the inhibitory action of DA on GABAergic transmission.

Presynaptic mechanism of DA on inhibitory transmission

Effect of DA on miniature IPSCs

To examine directly whether the effect of DA on evoked IPSCs is mediated by a presynaptic mechanism, its action on mIPSCs was analyzed. MBF neurons exhibited spontaneous IPSCs in the presence of TTX (0.5 μM), so they were probably true mIPSCs. The frequency of mIPSCs was rather low for analysis in the normal (2.5 mM CaCl_2) Krebs solution. Therefore, the baseline frequency of mIPSCs was increased by raising the external Ca^{2+} concentration to 7.5 mM in the presence of 0.5 μM TTX and 5 μM CNQX, as shown in Figure 5*A*. The mean frequency of mIPSCs under these conditions was 0.61 ± 0.11 Hz ($n = 11$). The cell illustrated in Figure 5 had a mean mIPSC amplitude of 18.8 ± 0.52 pA ($n = 190$ events), as indicated in the amplitude histogram [Fig. 5*C(a)*]. There was no significant correlation between rise time (10–90%) and mIPSC amplitude [Fig. 5*C(b)*], suggesting genuine variability in mIPSC amplitude rather than spatial dispersion. These mIPSCs were blocked by 10 μM bicuculline (data not shown). The mean frequency of mIPSCs was reduced after 1 min exposure of 10 μM DA and reached a steady level after 3 min (Fig. 5*B*). The amplitude histogram [Fig. 5*D(a)*] shows a 57.4% reduction in the total number of events, with no change in the mean amplitude of mIPSCs (16.9 ± 1.12 pA; $n = 81$ events) compared with the control value of 18.8 pA. The relationship between rise time and amplitude of mIPSCs also remained unchanged during DA application [Fig. 5*D(b)*]. Pooled data from six cells showed that 10 μM DA reduced the frequency of mIPSC by $64.8 \pm 2.1\%$, with no change in mean amplitude ($102.4 \pm 11.5\%$ of their respective controls). The mean rise time and the mean decay time constant of mIPSCs remained essentially the same during DA (10 μM) application ($104.0 \pm 3.9\%$ and $106.3 \pm 6.1\%$, respectively, of their controls). As shown in Figure 5*A,B*, DA (10 μM) reduced the

baseline noise level in most of the neurons tested; however, we did not investigate this phenomenon further in the present study.

To determine the contribution of voltage-sensitive calcium channels at GABAergic presynaptic terminals to DA-induced reduction of the inhibitory transmission, the effect of DA on mIPSCs in the presence of 100 μM cadmium (Cd^{2+}), a calcium channel blocker, was studied. This concentration of Cd^{2+} has been reported to block presynaptic calcium channels (Umehiya and Berger, 1995). The results of these experiments are expressed as amplitude histograms and depicted in Figure 6*A*. In the presence of Cd^{2+} , the frequency of mIPSCs was reduced without affecting their mean amplitudes, and in five cells tested, a mean reduction to $60.7 \pm 5.9\%$ of their respective controls was observed. This finding suggests an apparent contribution of Cd^{2+} -sensitive calcium influx to the spontaneous GABA release. Even in the presence of 100 μM Cd^{2+} (Fig. 6*C*), however, application of DA (10 μM) still reduced the frequency of mIPSCs, with a mean reduction by $52.3 \pm 7.1\%$ ($n = 5$), which was not significantly ($p > 0.18$) different from the effect of DA in the absence of Cd^{2+} ($64.8 \pm 2.1\%$; $n = 6$).

DISCUSSION

The main findings in the present study are that DA inhibits GABAergic inhibitory transmission onto MBF neurons via presynaptic D_1 -like receptors and that DA-induced presynaptic effect is independent of Ca^{2+} entry from outside and may be mediated by a cAMP-dependent pathway.

Although the inhibition produced by DA on the frequency of mIPSCs, without affecting their mean amplitude, strongly suggests that DA acts presynaptically, the exact origin of the inhibitory synapses that contribute to the mIPSC distributions remains to be established. Previous morphological studies have demonstrated that GABAergic terminals make synaptic contacts with neurons in the basal forebrain region (Zaborszky et al., 1986; Chang et al., 1995) and that a large proportion of these terminals probably arise from the nucleus accumbens (Heimer et al., 1991; Zaborszky and Cullinan, 1992). The IPSCs recorded in the present study may therefore be evoked by stimulating these fibers, although some of the IPSCs might also be evoked by direct stimulation of GABAer-

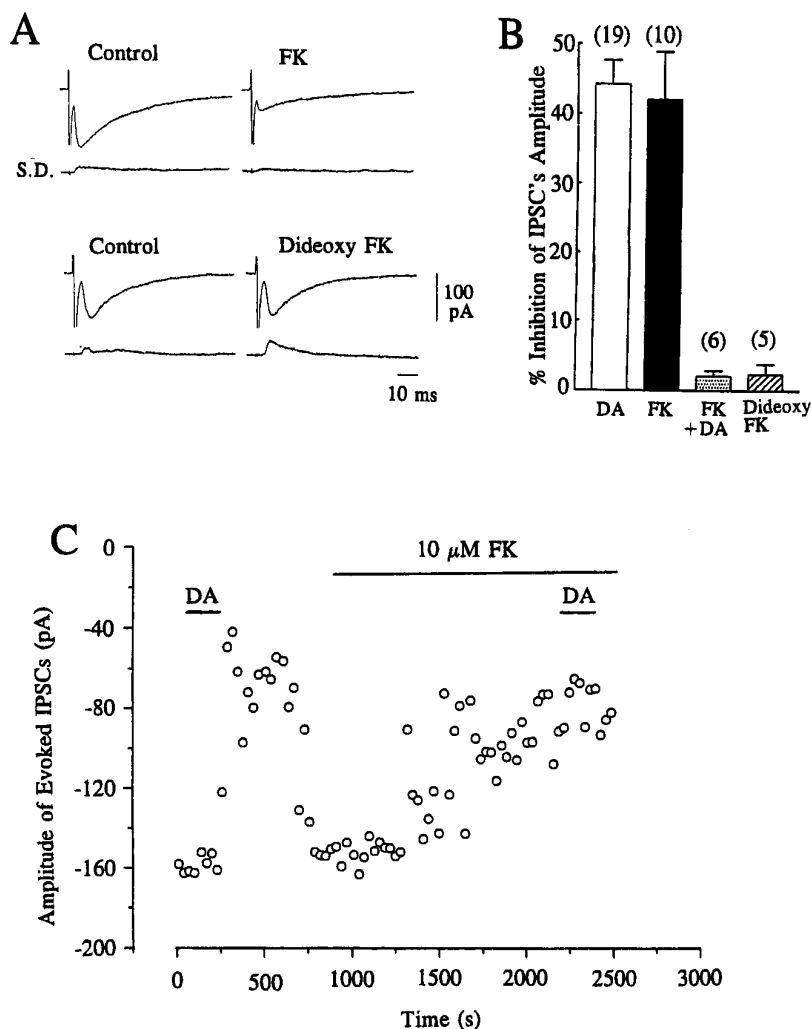


Figure 4. Effects of forskolin and 1,9-dideoxyforskolin on evoked IPSCs. *A*, Traces of evoked IPSCs showing the effect of forskolin (*FK*) and 1,9-dideoxyforskolin (*Dideoxy FK*). Each trace is the average of 10 consecutive responses evoked at 0.1 Hz with the corresponding SD. Current traces showing the effect of *FK* and dideoxy *FK* were derived from different cells. *B*, Summary histograms representing mean \pm SEM of % inhibition of the amplitude of IPSCs by dopamine (*DA*, 10 μ M), by *FK* (10 μ M), by *DA* subsequent to 10–20 min perfusion of *FK* (*FK+DA*), and by *Dideoxy FK*. Values were $44.3 \pm 3.4\%$ ($n = 19$), $42.1 \pm 6.8\%$ ($n = 10$), $2.1 \pm 0.76\%$ ($n = 6$), and $2.4 \pm 1.5\%$ ($n = 5$), respectively. (The value for *DA* was derived from the concentration–response curve in Fig. 1.) There was no significant ($p > 0.33$) difference in the effect produced by *DA* compared with *FK*. The dideoxy *FK*-induced effect was significantly ($p < 0.002$) smaller than that of *DA* or *FK*. Application of 10 μ M *DA* after the effect of *FK* had reached a steady level (after 15–20 min) produced virtually no further effect on the inhibitory action on the amplitude of IPSCs, and the effect of *DA* in the presence of *FK* was significantly ($p < 0.001$) smaller than that of *DA* or *FK* applied alone. *C*, Time course of the inhibitory effect of *FK* (10 μ M) on the amplitude of evoked IPSCs and occlusion of the effect of *DA* (10 μ M) in the continuing presence of *FK*. IPSCs were evoked at 0.1 Hz, and each point represents the mean amplitude of three consecutive responses. The holding potential was -70 mV.

gic neurons within basal forebrain nuclei, because some of the GABAergic terminals onto cholinergic neurons may arise from the local collaterals of intrinsic GABAergic neurons (Sun and Cassell, 1993).

The presynaptic inhibition of mIPSCs by *DA* remained unaffected in the presence of Cd^{2+} , suggesting that *DA* produces its inhibitory effect on the release of GABA subsequent to calcium entry via voltage-sensitive calcium channels. Similar calcium-independent mechanisms to presynaptic inhibition have been observed in other brain regions, namely the inhibition of excitatory transmission by activation of muscarinic and metabotropic glutamate receptors in the hippocampus (Scanziani et al., 1995), GABA_B receptors at a cerebellar synapse (Dittman and Regehr, 1996), and adenosine A₁ receptors in the hippocampus (Scholz and Miller, 1992), as well as in the reduction of inhibitory glycinergic transmission by the activation of 5-HT_{1B} receptors in the brain stem (Umehiya and Berger, 1995). In addition, a recent study has reported that activation of adenosine, GABA_B, or μ -opioid receptors inhibits ionomycin, gadolinium or α -latrotoxin-induced glutamate, and GABA release in a calcium-independent pathway (Capogna et al., 1996).

The present pharmacological results indicate that *DA* reduces inhibitory GABAergic synaptic transmission onto MBF neurons by a presynaptic mechanism that involves the activation of *DA* receptors with properties in common with D₁ family, most notably

from the antagonism by R(+)-SCH 23380. Although the apparent K_B value for R(+)-SCH 23390, a D₁-like antagonist, in the present study (0.82 μ M) is higher than the binding constant for [³H]SCH 23390 to cloned D₁ receptors (0.3–0.35 nM; cf. Sunahara et al., 1991) by three orders of magnitude, this antagonist has also been reported to show a 100-fold higher K_B value (40 nM) against the functional (cyclase-stimulating) action of *DA* than that predicted from its binding constant in broken membrane preparations (Andersen et al., 1985). In addition, 1–100 μ M of this antagonist was required to antagonize *DA*- or D₁-like agonist-induced effect in previous electrophysiological studies using rat brain slices as well as cultured neurons, while still preserving selectivity over D₂-like antagonists (Pennartz et al., 1992; Schiffmann et al., 1995; Harvey and Lacey, 1996; Nicola et al., 1996). Furthermore, another electrophysiological study using *Helix* has reported an estimated pA₂ value for SCH 23390 of 6.1 (Holden-Dye and Walker, 1989) at pharmacologically characterized D₁-like receptors, which is comparable with our estimated pK_B value. This requirement for higher concentrations in functional studies than those predicted by radioligand binding assays, coupled with the lesser effect of D₂-like agonist and antagonist, indicates that the effect of R(+)-SCH 23390 in the present study can be attributed to a block of D₁-like receptors rather than to any cross-reactivity with D₂-like receptors.

In our studies using agonists, however, namely R(-)-TNPA or

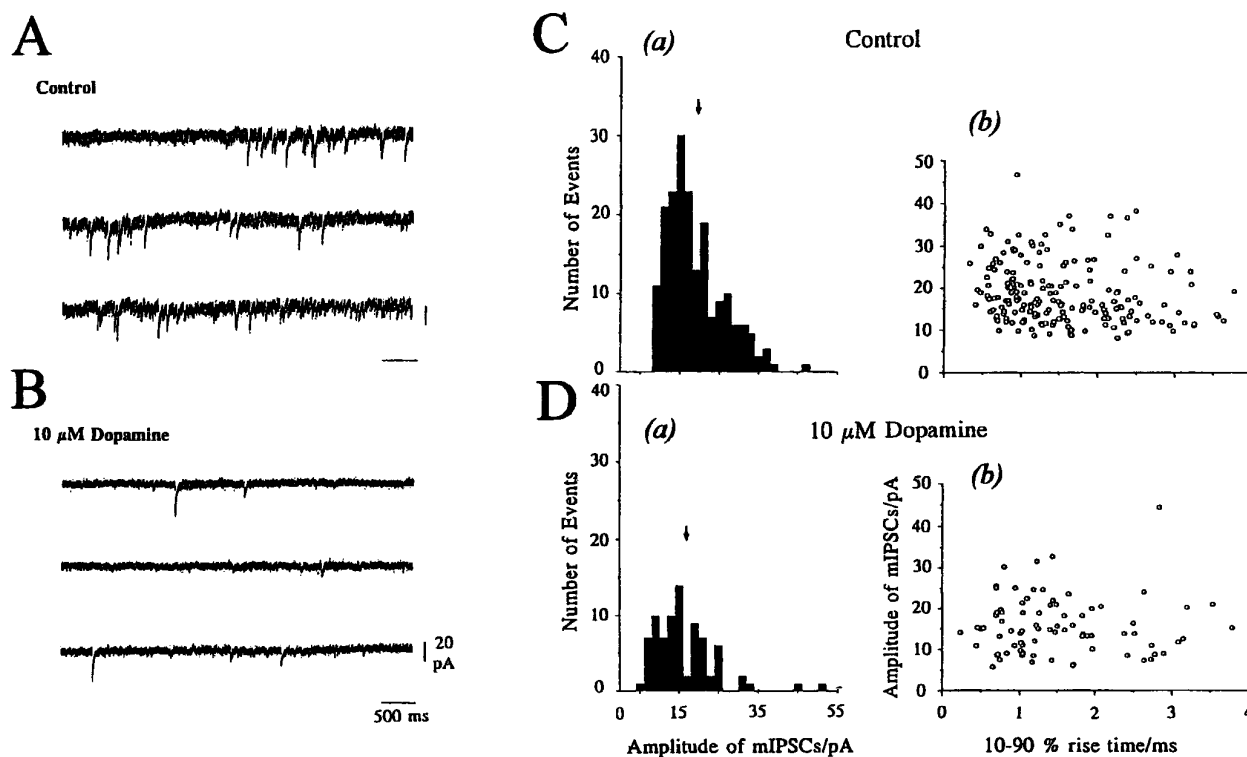


Figure 5. Effect of dopamine on spontaneous mIPSCs. mIPSCs were recorded in 7.5 mM external CaCl_2 Krebs solution containing TTX ($0.5 \mu\text{M}$) and CNQX ($5 \mu\text{M}$). *A, B*, Consecutive traces taken in control (*A*) and 3 min after application of $10 \mu\text{M}$ dopamine (*B*). Note that DA ($10 \mu\text{M}$) reduced the baseline noise level. *C(a), D(a)*, Amplitude histograms derived from 4 min stretches (bin width, 2.0 pA) of mIPSCs in control [*C(a)*, 190 events] and dopamine [*D(a)*, 81 events] sampled 3–7 min after application of dopamine. Arrows indicate the mean amplitude of mIPSCs (18.8 pA in control and 16.9 pA after application of dopamine). *C(b), D(b)*, Rise time (10–90%)/amplitude relation of mIPSCs before [*C(b)*] and after application of dopamine [*D(b)*]. *Control*: mean rise time = 3.03 ± 0.11 msec; mean decay time constant = 12.66 ± 0.55 msec. *Dopamine*: mean rise time = 3.02 ± 0.18 msec; mean decay time constant = 14.78 ± 0.89 msec. The holding potential was -70 mV.

(–)-quinpirole, these D_2 -like agonists had little or no effect on the amplitude of IPSCs. In contrast, the use of S(–)-eticlopride, a D_2 -like antagonist, induced a small antagonism on the concentration–response curve to DA. Because S(–)-eticlopride did not display any apparent antagonism to DA-mediated inhibition of excitatory transmission within these nuclei (Momiya et al., 1996), the present finding seemed to suggest that a possible (but to a lesser extent) contribution of D_2 -like receptors to the depression of evoked IPSCs cannot be excluded completely. In the present study, however, simultaneous application of both D_1 -like and D_2 -like agonists showed no different effect from that induced by D_1 -like agonist alone, indicating no apparent interaction between D_1 -like and D_2 -like receptors.

One interesting finding of the present study is the observation that the application of forskolin reduced the amplitude of the evoked IPSCs by itself. This action of forskolin occluded the inhibitory effect of DA on IPSCs, because DA applied in the presence of forskolin evoked no further reduction in the amplitude of evoked IPSCs. Because forskolin stimulates adenylate cyclase and increases $[\text{cAMP}]_i$ levels, and D_1 -like receptors have been classified as those positively coupled to adenylate cyclase activity (Kebabian and Calne, 1979), these results provide further support for the role of D_1 -like receptors for the inhibition of GABAergic inhibitory transmission. The present finding that forskolin inhibits IPSCs in MBF neurons, however, contrasts with previous studies at other synapses where forskolin has been reported to enhance inhibitory synaptic transmission (Llano and Gerschenfeld, 1993; Capogna et al., 1995). One possible explana-

tion for this opposing action of forskolin may be explained by differences in presynaptic mechanisms in different brain regions under study, but additional studies are necessary to clarify the precise mechanisms.

Although D_1 -like receptor-mediated facilitation of GABA release has been reported in putative DA-containing neurons in the ventral tegmental area (Cameron and Williams, 1993), the present finding that D_1 -like receptors are involved in mediating inhibition of the release of GABA to increase cellular excitability within basal forebrain nuclei correlates well with data of a previous report that DA attenuated the inhibitory action of iontophoretic application of GABA (Bergstrom and Walters, 1984). On the other hand, presynaptic D_1 -like receptors have also been reported to be involved in the inhibition of excitatory transmission in these basal forebrain neurons (Momiya et al., 1995a; 1996) as well as in nucleus accumbens (Pennartz et al., 1992; Harvey and Lacey, 1996; Nicola et al., 1996). The role of D_1 -like receptors in modulating both excitatory and inhibitory inputs onto magnocellular neurons suggests that DA has a role in regulating the balance between excitation and inhibition within basal forebrain nuclei. Indeed, such dual actions of DA is reflected in the findings of a previous electrophysiological study using anesthetized rats (Napier and Maslowski-Cobuzzi, 1994) in which neuronal activity in the ventral pallidum can be variably inhibited or excited by iontophoretic application of DA.

In conclusion, the results of the present study strongly suggest that DA projections to basal forebrain nuclei play an important role in controlling the activity of inhibitory transmission onto

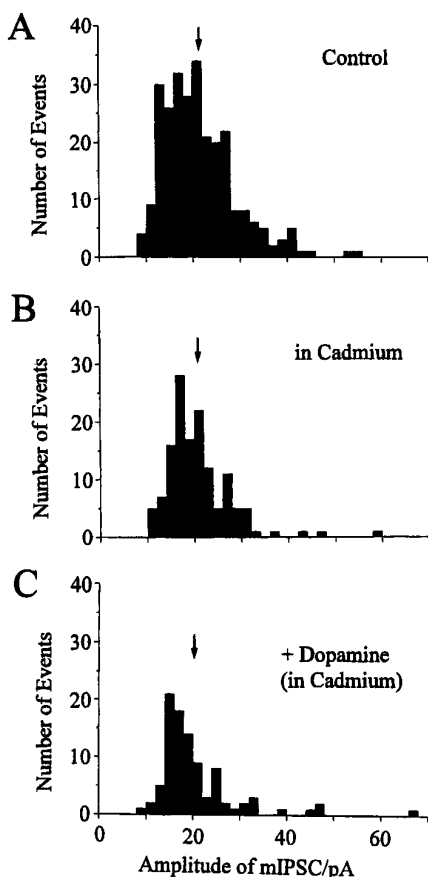


Figure 6. Effect of cadmium on mIPSCs. Amplitude histograms derived from 4 min stretches (bin width, 2.0 pA) in control (*A*, 267 events), in the presence of 100 μM cadmium (*B*, 138 events), and after 10 μM dopamine (*C*, 94 events) in the continuing presence of cadmium. Arrows indicate the mean amplitudes of mIPSCs in control, in cadmium, and in dopamine/cadmium (21.5, 20.7, and 20.5 pA, respectively). mIPSCs were recorded in 7.5 mM CaCl_2 , 0.5 μM TTX, and 5 μM CNQX at a holding potential of -70 mV.

cholinergic basal forebrain neurons to increase cellular excitability. Coupled with our previous findings on excitatory transmission (Momiya et al., 1996), however, the action of DA is neither an “excitatory” nor an “inhibitory” transmitter in basal forebrain nuclei. Indeed, the dopaminergic inputs terminating onto magnocellular neurons seemed to play more of a role in controlling the balance between excitatory and inhibitory synaptic circuitry of these cortically projecting nuclei. From a pathophysiological point of view, the present findings also raise the possibility that dopaminergic systems might also be involved in some of the defects in cognition and memory in various neurodegenerative diseases, including Alzheimer’s disease or senile dementia, as well as Parkinson’s disease, schizophrenia, or drug abuse.

REFERENCES

Andersen PH, Jansen JA (1990) Dopamine receptor agonists: selectivity and dopamine D_1 receptor affinity. *Eur J Pharmacol* 188:335–347.
 Andersen PH, Gronvald FC, Jansen JA (1985) A comparison between dopamine-stimulated adenylate cyclase and ^3H -SCH 23390 binding in rat striatum. *Life Sci* 37:1971–1983.
 Bergstrom DA, Walters JR (1984) Dopamine attenuates the effect of GABA on single unit activity in the globus pallidus. *Brain Res* 310:23–33.
 Cameron DL, Williams JT (1993) Dopamine D_1 receptors facilitate transmitter release. *Nature* 366:344–347.

Capogna M, Gähwiler BH, Thompson SM (1995) Presynaptic enhancement of inhibitory synaptic transmission by protein kinase A and C in the rat hippocampus *in vitro*. *J Neurosci* 15:1249–1260.
 Capogna M, Gähwiler BH, Thompson SM (1996) Presynaptic inhibition of calcium-dependent and -independent release elicited with ionomycin, gadolinium, and α -latrotoxin. *J Neurophysiol* 75:2017–2028.
 Chang HT, Tian Q, Herron P (1995) GABAergic axons in the ventral forebrain of the rat: an electron microscopic study. *Neuroscience* 68:207–220.
 Coyle JT, Price DL, DeLong MR (1983) Alzheimer’s disease: a disorder of cortical cholinergic innervation. *Science* 219:1184–1190.
 Dittman JS, Regehr WG (1996) Contribution of calcium-dependent and calcium-independent mechanisms to presynaptic inhibition at a cerebellar synapse. *J Neurosci* 16:1623–1633.
 Eaton MJ, Wagner CK, Moore KE, Lokkingland KJ (1994) Neurochemical identification of A_{13} dopaminergic neuronal projections from the medial zona interna to the horizontal limb of the diagonal band of Broca and the central nucleus of the amygdala. *Brain Res* 659:201–207.
 Gao Y, Baldessarini RJ, Kula NS, Neumeier JL (1990) Synthesis and dopamine receptor affinities of enantiomers of 2-substituted apomorphines and their *N-n*-propyl analogues. *J Med Chem* 33:1800–1805.
 Hall H, Kohler C, Gawell L (1985) Some *in vitro* receptor binding properties of [^3H]-eticlopride, a novel substituted benzamide, selective for dopamine D_2 receptors in the rat brain. *Eur J Pharmacol* 111:191–199.
 Harvey J, Lacey MG (1996) Endogenous and exogenous dopamine depress EPSCs in rat nucleus accumbens *in vitro* via D_1 receptor activation. *J Physiol (Lond)* 492:143–154.
 Heimer L, Zahm DS, Churchill L, Kalivas PW, Wohtmann C (1991) Specificity in the projection patterns of accumbal core and shell in the rat. *Neuroscience* 41:89–125.
 Holden-Dye L, Walker RJ (1989) Further characterization of the dopamine-inhibitory receptor in *helix* and evidence for a noradrenaline-preferring receptor. *Comp Biochem Physiol* 93C:413–419.
 Iorio LC, Barnett A, Leitz FH, Houser VP, Korduba CA (1983) SCH 23390, a potential benzazepine antipsychotic with unique interactions on dopaminergic system. *J Pharmacol Exp Ther* 226:462–468.
 Jonas P, Major G, Sakmann B (1993) Quantal components of unitary EPSCs at the mossy fibre synapse on CA3 pyramidal cells of rat hippocampus. *J Physiol (Lond)* 472:615–663.
 Keibadian JW, Calne DB (1979) Multiple receptors for dopamine. *Nature* 277:93–96.
 Llano I, Gerschenfeld HM (1993) β -adrenergic enhancement of inhibitory synaptic activity in rat cerebellar stellate and Purkinje cells. *J Physiol (Lond)* 468:201–224.
 Martinez-Murillo R, Semenko F, Cuello AC (1988) The origin of tyrosine hydroxylase-immunoreactive fibers in the region of the nucleus basalis magnocellularis of the rat. *Brain Res* 451:227–236.
 Momiya T, Sim JA, Brown DA (1995a) Presynaptic inhibition of excitatory inputs to rat magnocellular basal forebrain neurones by dopamine. *J Physiol (Lond)* 487:P:50P.
 Momiya T, Sim JA, Brown DA (1995b) Dopaminergic inhibition of synaptic currents in cholinergic magnocellular neurons in the basal forebrain. *Soc Neurosci Abstr* 21:1091.
 Momiya T, Sim JA, Brown DA (1996) Dopamine D_1 -like receptor-mediated presynaptic inhibition of excitatory transmission onto rat magnocellular basal forebrain neurones. *J Physiol (Lond)* 495:97–106.
 Napier TC, Malowski-Cobuzzi RJ (1994) Electrophysiological verification of the presence of D_1 and D_2 dopamine receptors within the ventral pallidum. *Synapse* 17:160–166.
 Nicola SM, Kombian SB, Malenka RC (1996) Psychostimulants depress excitatory synaptic transmission in the nucleus accumbens via presynaptic D_1 -like dopamine receptors. *J Neurosci* 16:1591–1604.
 Oyanagi K, Takahashi H, Wakabayashi K, Ikuta F (1989) Correlative decrease of large neurons in the neostriatum and basal nucleus of Meynert in Alzheimer’s disease. *Brain Res* 504:354–357.
 Pennartz CMA, Dolleman-Van Der Weel MJ, Kitai ST, Lopes Da Silva FH (1992) Presynaptic dopamine D_1 receptors attenuate excitatory and inhibitory limbic inputs to the shell region of the rat nucleus accumbens studied *in vitro*. *J Neurophysiol* 67:1325–1334.
 Rye DB, Wainer BH, Mesulam M-M, Mufson EJ, Saper CB (1984) A study of cholinergic and noncholinergic components employing combined retrograde tracing and immunohistochemical localization of choline acetyltransferase. *Neuroscience* 13:627–643.
 Scanziani M, Gähwiler BH, Thompson SM (1995) Presynaptic inhibition of excitatory synaptic transmission by muscarinic and metabotropic

- glutamate receptor activation in the hippocampus: are Ca^{2+} channels involved? *Neuropharmacology* 34:1549-1557.
- Schiffmann SN, Lledo P-M, Vincent J-D (1995) Dopamine D_1 receptor modulates the voltage-gated sodium current in rat striatal neurones through a protein kinase A. *J Physiol (Lond)* 483:95-107.
- Scholz KP, Miller RJ (1992) Inhibition of quantal transmitter release in the absence of calcium influx by a G protein-linked adenosine receptor at hippocampal synapses. *Neuron* 8:1139-1150.
- Semba K, Reiner PB, McGeer EG, Fibiger HC (1988) Brainstem afferents to the magnocellular basal forebrain studied by axonal transport, immunohistochemistry, and electrophysiology in the rat. *J Comp Neurol* 267:433-453.
- Sim JA (1994) Maintained morphology of rat magnocellular cholinergic basal forebrain neurones in culture. *J Physiol (Lond)* 480.P:34P.
- Sim JA, Griffith WH (1996) Muscarinic inhibition of glutamatergic transmission onto rat magnocellular basal forebrain neurones in a thin-slice preparation. *Eur J Neurosci* 8:880-891.
- Stern P, Edwards FA, Sakmann B (1992) Fast and slow components of unitary EPSCs on stellate cells elicited by focal stimulation in slices of rat visual cortex. *J Physiol (Lond)* 449:247-278.
- Sun N, Cassell MD (1993) Intrinsic GABAergic neurons in the rat central extended amygdala. *J Comp Neurol* 330:381-404.
- Sunahara RK, Guan H-C, O'Dowd BF, Seeman P, Laurier LG, Gordon NG, George SR, Torchia J, Van Tol HHM, Niznik HB (1991) Cloning of the gene for a human dopamine D_5 receptor with higher affinity for dopamine than D_1 . *Nature* 350:614-619.
- Takahashi T (1992) The minimal inhibitory synaptic currents evoked in neonatal rat motoneurons. *J Physiol (Lond)* 450:593-611.
- Titus RD, Korndeld EC, Jones ND, Clemens JA, Smalstig EB, Fuller RW, Hahn RA, Hynes MD, Mason NR, Wong DT, Foreman MM (1983) The resolution and absolute configuration of an ergoline-related dopamine agonist, trans-4,4a5,6,7,8,8a,9-octahydro-5-propyl-1H-pyrazolo[3,4-g]quinoline. *J Med Chem* 26:1112-1116.
- Umamiya M, Berger AJ (1995) Presynaptic inhibition by serotonin of glycinergic inhibitory synaptic currents in the rat brain stem. *J Neurophysiol* 73:1192-1200.
- Zaborszky L, Cullinan WE (1992) Projections from the nucleus accumbens to cholinergic neurons of the ventral pallidum: a correlated light and electron microscopic double-immunolabeling study in rat. *Brain Res* 570:92-101.
- Zaborszky L, Heimer L, Eckenstein F, Leranth C (1986) GABAergic input to cholinergic forebrain neurons: an ultrastructural study using retrograde tracing of HRP and double immunolabeling. *J Comp Neurol* 250:282-295.